



Historical reconstruction of the Atlantic Meridional Overturning Circulation from the ECMWF operational ocean reanalysis

Magdalena Balmaseda, Gregory Smith, Keith Haines, David Anderson, Tim Palmer, Arthur Vidard

► To cite this version:

Magdalena Balmaseda, Gregory Smith, Keith Haines, David Anderson, Tim Palmer, et al.. Historical reconstruction of the Atlantic Meridional Overturning Circulation from the ECMWF operational ocean reanalysis. *Geophysical Research Letters*, American Geophysical Union, 2007, 34 (23), pp.L23615. 10.1029/2007GL031645 . inria-00181739

HAL Id: inria-00181739

<https://hal.inria.fr/inria-00181739>

Submitted on 24 Oct 2007

HAL is a multi-disciplinary open access archive for the deposit and dissemination of scientific research documents, whether they are published or not. The documents may come from teaching and research institutions in France or abroad, or from public or private research centers.

L'archive ouverte pluridisciplinaire **HAL**, est destinée au dépôt et à la diffusion de documents scientifiques de niveau recherche, publiés ou non, émanant des établissements d'enseignement et de recherche français ou étrangers, des laboratoires publics ou privés.

1 **Historical reconstruction of the Atlantic Meridional Overturning** 2 **Circulation from the ECMWF operational ocean reanalysis**

3 Magdalena A. Balmaseda¹, Gregory C. Smith², Keith Haines², David Anderson¹, T.N.
4 Palmer¹ and Arthur Vidard³

5 ¹European Centre for Medium Range Weather Forecasts, Shinfield Park, Reading RG2
6 9AX, UK.

7 ²ESSC, Harry Pitt Bld, Earley Gate, Reading University, Reading RG6 6AL, UK.

8 ³INRIA, LJK - B.P. 53 - 38041 - Grenoble cedex 9, France.

9 A reconstruction of the Atlantic Meridional Overturning Circulation (MOC) for the
10 period 1959-2006 has been derived from the ECMWF operational ocean reanalysis. The
11 reconstruction shows a wide range of time-variability, including a downward trend. At
12 26N, both the MOC intensity and changes in its vertical structure are in good agreement
13 with previous estimates based on trans-Atlantic surveys. At 50N, the MOC and strength
14 of the subpolar gyre are correlated at interannual time scales, but show opposite secular
15 trends. Heat transport variability is highly correlated with the MOC but shows a smaller
16 trend due to the warming of the upper ocean, which partially compensates for the
17 weakening of the circulation. Results from sensitivity experiments show that although
18 the time-varying upper boundary forcing provides useful MOC information, the
19 sequential assimilation of ocean data further improves the MOC estimation by
20 increasing both the mean and the time variability.

21 **1. Introduction**

22 The Atlantic meridional overturning circulation (MOC) is composed of a warm
23 near-surface branch flowing northward as part of the Gulf Stream and a return flow of
24 cold waters at depth. It plays a major role in the heat transport of the ocean, in turn

25 affecting the climate of Europe and North America (e.g. Cubash et al 2001), and its
26 variability plays an important role in future climate change scenarios. However, reliable
27 estimates and understanding of the variability remain elusive. Bryden et. al. (2005),
28 (hereafter BLC05) using density measurements from five transatlantic research cruises
29 at approximately 26°N between 1957-2004, found a 30% decrease in MOC intensity,
30 with a notable reduction in the southward flow of the lower North Atlantic Deep Water
31 (NADW) coming from high latitudes, although these conclusions were based on very
32 limited temporal sampling. In contrast, estimates relying on ocean model simulations
33 have produced an intensification of the MOC (e.g. Böning et. al. 2006), which could be
34 attributed to the prevailing positive phase of the North Atlantic Oscillation (NAO) since
35 1980's (Eden and Willebrand (2001)).

36 The contradictory results between observational and model estimates illustrate the
37 underlying uncertainties in the different methodologies: the observational BLC05 data
38 clearly have insufficient temporal sampling to estimate trends, and the model results can
39 be affected by errors in the forcing fluxes and model formulation. A hybrid approach is
40 the synthesis of ocean model and observations using data assimilation techniques, to
41 produce an ocean analysis (for a summary of ongoing activities see
42 <http://www.clivar.org/organization/gsop/synthesis/synthesis.php>). In theory, the error in
43 the MOC from an ocean analysis should be smaller than the errors in ocean model or
44 observational estimates alone. In practice, some new uncertainties may be introduced
45 from different assimilation techniques or observations of varying density/accuracy.

46 Ocean analyses such as ECCO have previously been used to derive
47 reconstructions of the MOC (Wunsch and Heimbach (2006) and Köhl and Stammer
48 (2007)). These ECCO analyses are based on long-window adjoint methods, and
49 typically rely on the correction of the ocean initial conditions and surface forcing to get
50 close to the observed ocean data. Here we present a 48 year historical reconstruction of

51 the MOC (for the period 1959-2006) from the ECMWF operational ocean reanalysis
52 System 3 (ORAS3 in what follows), which uses a sequential assimilation method to
53 directly correct the density field, which is critical to circulation indices such as the
54 MOC.

55 The paper is organized as follows: we describe the ocean analysis system, and the
56 sensitivity experiments in secn 2, the reconstruction of the MOC, including the
57 meridional and vertical structure in secn 3 and the implications for the meridional heat
58 transports in secn 4. Results from sensitivity experiments are presented in secn 5 and
59 conclusions in secn 6.

60 **2 The data assimilation system**

61 The analysis of the ocean state is obtained by integrating a global ocean model with
62 atmospheric surface fluxes acting as time-dependent upper boundary conditions. The
63 ocean model is HOPE (Wolff et al. 1997, Balmaseda 2004), $1^\circ \times 1^\circ$ resolution, with a
64 tropical enhancement to $1/3^\circ$, and 29 vertical levels, with partial step topography and
65 explicit free surface. From 1959 to August 2002, the forcing fluxes are from the
66 ERA40 atmospheric reanalysis with corrected freshwater fluxes, and from the
67 operational atmospheric analysis thereafter (ERA40/OPS in what follows). The ocean
68 observations are assimilated sequentially via an optimal interpolation (OI) method,
69 which imposes dynamical and physical constraints. The analysis cycle is repeated every
70 10 days. A detailed description of the system is given in Balmaseda et al 2007a.

71 The subsurface observations consist of vertical profiles of temperature and salinity from
72 Bathythermographs (MBT, XBT) , Conductivity Temperature Depth (CTD) sensor measurements
73 from scientific cruises, TAO/TRITON and PIRATA moorings, and more recently Argo floats.
74 Historical salinity data are scarce, and it is only with the advent of Argo floats that a near-global
75 coverage of salinity observations is available (from 2000 onwards). For the period 1959-2004 the

76 subsurface data are from the comprehensive quality-controlled data set ENACT-ENSEMBLES
77 (Ingleby and Huddleston, 2006) , which contains 5.1 million temperature and 1.4 million salinity
78 profiles. From 2005 onwards, the subsurface data are from the ECMWF operational archive, and
79 are subject to a different automatic quality control procedure. For the later period, a typical 10-day
80 assimilation window contains 2500 profiles of temperature and 1100 profiles of salinity. Maps of
81 sea surface temperature (Reynolds et al 2002) are also assimilated and, from 1993 onwards,
82 satellite-derived sea level anomaly maps (Le Traon et al 1998) are used. Supplementary figure 1
83 shows a timeseries of the number of temperature profile observations used in a 10-day
84 assimilation cycle in the North Atlantic (20N-50N) as a function of depth. The observation
85 coverage maps for the individual assimilation cycles can be seen at
86 <http://www.ecmwf.int/products/forecasts/d/charts/ocean/reanalysis/obsmap/>.

87 The ORAS3 is part of the operational monthly and seasonal forecasting system, where a
88 reliable reconstruction of the time variability of the ocean is required to improve the
89 skill of the system. Special attention has been paid to the tuning of the error
90 covariances, where the correlation scales and the diagonal elements have been chosen
91 so as to improve both the mean state and the interannual variability. In addition, to
92 reduce spurious time-variability resulting from the changing nature of the observing
93 system, ORAS3 uses low frequency bias-corrections to both the pressure gradient and
94 the temperature and salinity fields (Balmaseda et al 2007b). Only a weak relaxation to
95 the full temperature and salinity climatology is used (10-year time scale), which does
96 not significantly damp the interannual variability.

97 To assess the impact of assimilating data, a control experiment (ORA-nobs) is
98 conducted by integrating the ocean model with the ERA40/OPS fluxes but without
99 assimilating profiles or altimeter data. Everything else (spin up, relaxation to SST and
100 3D climatology) is the same as in ORAS3. To assess the impact of the forcing fluxes
101 and spin up an additional experiment is conducted, identical to ORA-nobs but using a

102 climatology of the daily fluxes as forcing. The effect of initial conditions on the MOC
103 in ORAS3 at the beginning of the record is explored by a set of 10-year assimilation
104 experiments starting from perturbed initial conditions in 1956.

105 **3. The historical reconstruction of the MOC**

106 Balmaseda et al 2007a show that the ORAS3 reanalysis is consistent with the
107 observed profile data, and quantitatively reproduces the expected mean circulations and
108 time variations in temperature, salinity and surface currents. The Atlantic meridional
109 heat transports in ORAS3 are in good agreement with WOCE estimates (Ganachaud
110 and Wunsch 2003, supplementary table1). Figure 1 shows the Atlantic MOC at 26°N
111 for ORAS3, calculated by integrating the zonal-mean velocity from the surface to
112 1200m (chosen as the depth of maximum overturning in the model). The agreement
113 between ORAS3 and the BLC05 values is remarkably good for 1981, 1992 and 1998,
114 but differs in 2004, where the BLC05 value is substantially lower. However, more
115 recent estimates from the RAPID array (Cunningham et al 2007) yield an average MOC
116 value of 18.7Sv for 2004, which is in good agreement with ORAS3. Although the
117 agreement is very encouraging, one should remember that there are only four points and
118 there are likely substantial uncertainties in both the section/array estimates and model
119 values.

120 Figure 1 also indicates the large seasonal (1.8 Sv) and interannual (1.9Sv) variability of
121 the MOC. The seasonal variability of the MOC at 26°N can be attributed mainly to the
122 seasonality of the Ekman transport, which has a standard deviation of 1.9Sv. Ekman
123 transport makes up about 25% of the time-mean and interannual transports (4.9 Sv and
124 0.56 Sv respectively). The MOC at 26°N in ORAS3 shows a small decrease over the
125 48-year period which amounts to -0.07 ± 0.01 Sv/yr, equivalent to a reduction of 4%
126 per decade, although from figure 1 it is clear that this trend is not constant (e.g. the trend

127 after the mid-1970's is only 2% per decade). The weakening MOC is associated with
128 changes in vertical structure of the circulation (figure 2a). Consistent with BLC05, there
129 is a reduction in the southward transport of the lower North Atlantic Deep Water
130 (NADW) in ORAS3, associated with a shallower and weaker recirculation cell. This is
131 an important difference from the 11-year ECCO-GODAE reanalysis (Wunsch and
132 Heimbach, 2006), which also shows a slow-down of the MOC, but with an
133 intensification of the southward NADW flow. (The differences between ORAS3 and
134 ECCO-GODAE are likely to stem from the different assimilation methods). The
135 coherent changes in the vertical structure of the circulation occur at low frequency, and
136 do not seem to be affected by the seasonal variability of the Ekman transport. This
137 implies that vertical structure comparisons with BLC05 are more robust, since they are
138 not contaminated by high frequency variability.

139 Figure 2a also shows a reduction of the northward transport within the
140 thermocline which, according to Cunningham and Alderson 2007, results from an
141 intensified southward geostrophic transport caused by the increased east-west
142 thermocline slope, and is consistent with the changes in the vertical density structure in
143 ORAS3. There is a general warming and salinification in the upper subtropical ocean,
144 indicative of thermocline deepening, which is more pronounced in the western part of
145 the basin. ORAS3 also reproduces an increase in temperature and salinity (0.42 K and
146 0.07 psu respectively at 450m) in the Eastern Atlantic between 1992 and 2002, noted by
147 Vargas-Yáñez et al (2004) from a cruise survey at 24°N.

148

149 The time variability of the MOC in ORAS3 changes considerably as a function of
150 latitude (figure 2b). Within the subtropical gyre (south of 30N) the interannual
151 variability is dominant, while in subpolar latitudes decadal variability is stronger. A

152 reduction in the MOC (2-4% per decade, supplementary table 2 and supplementary
153 figure 4) is apparent in most of the North Atlantic domain, and is particularly
154 pronounced after 1995, with a visible reduction in the meridional extension of the
155 MOC. Häkkinen and Rhines (2004) attribute this reduction of the MOC after 1995 to
156 the weakening of the subpolar gyre (SPG), characterized by a decrease in sea level
157 gradients from satellite altimetry. The intensity of the SPG in ORAS3 (measured by the
158 sea level differences between 40N and 60N) is correlated with the MOC at 50N at
159 interannual time scales ($r=0.8$), in agreement with Böning et al (2006), with the MOC in
160 ORAS3 lagging the subpolar gyre by 18 months (figure 3). But contrary to other model
161 studies, the secular trends of the MOC and the SPG found here are of opposite sign.
162 There are several possible reasons for this: i) the atmospheric forcing fluxes (ORAS3
163 uses ERA40/OPS instead of NCEP) ii) the surface heat flux closure (in ORAS3 there is
164 strong relaxation to time-varying SST, which may compensate for errors in the heat
165 fluxes, thus contributing to a better simulation of the upper ocean warming); and iii) the
166 representation of the overflows. For instance, Böning et al (2006) impose climatological
167 boundary conditions at 70N, while ORAS3 overflow properties may vary in time and be
168 affected by the assimilation of ocean observations.

169 **4 Heat transports**

170 It has been suggested that any slowdown of the MOC could have significant
171 implications for the climate of Europe (Vellinga and Wood 2002) due to a resulting
172 reduction in heat transport in the northward flowing upper limb. In ORAS3, the
173 interannual variability in the heat transport at 26°N follows closely the MOC variability
174 (correlated at $r = 0.9$), and also shows a small downward trend of -0.0029 ± 0.0007
175 PW/yr, equivalent to a reduction of 2.7% per decade. This fractional trend in heat
176 transport is weaker than for the MOC over the whole North Atlantic domain
177 (supplementary table 2 and supplementary figure 4). This is a consequence of the

178 increased vertical temperature gradient resulting from a general upper ocean warming
179 (Fig. 4). At 26°N there is a modest warming trend in the upper 300 m of 0.05 ± 0.01
180 K/decade, while at 40°N this increases to 0.26 ± 0.04 K/decade. The increased upper
181 ocean temperatures in the poleward moving branch of the MOC intensify the poleward
182 heat transport, partially cancelling the effect of the weakening MOC, in agreement with
183 the simulations of Drijfhout and Hazeleger (2006).

184 **5. Sensitivity experiments**

185 The time variability of the MOC reconstruction could be affected by variations in
186 the observing system and spin-up effects. Here we use sensitivity experiments to assess
187 the robustness of the ORAS3 results. The agreement with the observed temperature and
188 salinity profiles is better for ORAS3 than for ORA-nobs (about 30% in the North
189 Atlantic, supplementary figure 2). The improved representation of the density field
190 affects both the mean overturning strength and the amplitude of the variability,
191 improving dramatically the agreement with the BLC05 values relative to the ORA-nobs
192 (fig 1), as well as the heat transports, which are underestimated in ORA-nobs
193 (supplementary table 1). The coherence between ORAS3 and ORA-nobs is also
194 apparent at 50N, where the MOC and the SPG intensity in ORA-nobs show positively
195 correlated interannual variability and opposite secular trends (not shown).

196 The large degree of coherence between the time evolution of the MOC in ORAS3
197 and ORA-nobs is indicative of the atmospherically-driven component. ORA-nobs
198 simulates the same large MOC values during the 60's, increased variability during the
199 80's, and the quasi-biennial signals after 2000. ORA-nobs also shows a decline in MOC
200 intensity, although of a smaller magnitude than ORAS3 (2% per decade), suggesting
201 that some trend is directly linked to changes in the atmospheric forcing. In contrast, the
202 experiment with climatological forcing (supplementary figure 3), shows no significant

203 trend after an initial adjustment, supporting the attribution of part of the MOC decline to
204 the time-varying upper boundary forcing.

205 Direct comparison with the BLC05 value for 1957, outside the ORAS3 record, is
206 not possible. Additional experiments, similar to ORAS3 but starting from 1956 were
207 conducted. Prior to 1958 there is no ERA40 forcing, and so climatological forcing was
208 used. Different ocean initial conditions were used: a) ORAS3 spin up, b) ORAS3 (1 Jan
209 1962) and c) ORAS3 (1 Jan 1965). None of these experiments reproduced the BCL05
210 MOC value for 1957, probably because of the scarcity of information (both
211 observational and forcing). Results also show that the MOC converges to the ORAS3
212 value by 1962, suggesting that the spin up is not a determining factor in ORAS3 after
213 1962.

214 Additional experiments show that the estimated MOC trend and the specific
215 agreement with the BLC05 values remain unchanged even if all the specific section data
216 used by BLC05 are withdrawn from the ORAS3 reanalysis. This illustrates the ability of
217 data assimilation systems to propagate observational information either directly, via the
218 prescribed error correlation functions, or via physical processes represented by the
219 ocean model.

220 **6. Summary**

221 These results show that assimilating data in ORAS3 improves the representation
222 of the Atlantic MOC against section-based estimates, and permits a 48-year
223 reconstruction, for the period 1959-2006, which exhibits a wide range of time
224 variability (seasonal, interannual and secular trends). ORAS3 results suggest a slow-
225 down of the MOC (2-4% per decade) for most of the North Atlantic basin, although the
226 trends are not constant, being much smaller in the second half of the record.

227 The MOC variability in the subtropical gyre is highly correlated with the heat
228 transport variability, but the trends in heat transport are weaker, due to slow changes in
229 the vertical thermal structure, with the pronounced upper ocean warming partially
230 compensating for the reduction in the MOC.

231 Sensitivity experiments suggest that either ERA40 atmospheric forcing and/or
232 the strong constraint on the SST can explain some of the reduction of the MOC, but that
233 the trend is enhanced by the assimilation of in situ ocean data. The results presented
234 here support the paradigm of the North Atlantic Oscillation (NAO) as providing the
235 primary forcing for the MOC at 50N on interannual timescales (Eden and Willebrand,
236 2001), with positive NAO conditions leading to the intensification of the MOC.
237 However, the reduction of the MOC at 50N in ORAS3 under prevailing positive NAO
238 conditions during recent decades, accompanied by the decline in the southward
239 transport of the lower NADW, suggest that other factors are more important for the
240 MOC on longer timescales.

241 These results illustrate the potential of ocean reanalysis for the study of ocean
242 climate. In the latest IPCC Assessment Report, it was stated that due to the conflict
243 between model and observational studies, “no coherent evidence” of a trend in the
244 MOC over the last 50 years existed, and hence no baseline comparison was possible for
245 climate model simulations. It is shown here that data assimilation can reconcile model
246 and observations, giving a self consistent MOC timeseries which agrees with traditional
247 section-based estimates where available. Sensitivity experiments can test robustness and
248 further reanalyses based on other models and methods are underway (within CLIVAR-
249 GSOP panel) that will further reduce the uncertainty in these estimations of the MOC.
250 Ocean reanalysis should be able to provide a past baseline for MOC estimates, and more
251 generally, a valuable gauge on the quality of climate models used for future climate

252 projections. The uncertainties in the ocean reanalysis will be reduced, as the quality of
253 the assimilation methods, ocean model and atmospheric reanalyses improves.

254

255 References.

256 Balmaseda, M.A., 2004: Ocean data assimilation for seasonal forecasts. ECMWF
257 Seminar Proceedings. Seminar on Recent developments in data assimilation for
258 atmosphere and ocean, 8-12 September 2003, 301-326.

259 Balmaseda, M., Vidard, A. & Anderson, D. 2007a. The ECMWF System 3 ocean
260 analysis system. ECMWF Technical Memorandum, 508.
261 (http://www.ecmwf.int/publications/library/ecpublications/_pdf/tm/501-600/tm508.pdf).

262 Balmaseda, M.A., D. Dee, A. Vidard and D.L.T. Anderson, 2007b. A Multivariate Treat
263 ment of Bias for Sequential Data Assimilation: Application to the Tropical Oceans. *Q. J. R. Meteorol. Soc.*, **133**, 167-179.

265 Bindoff, N.L. & Willebrand, J., 2007: Observations: Climate Change and Sea Level,
266 IPCC WG1 AR4 Final Report.
267 http://ipccwg1.ucar.edu/wg1/Report/AR4WG1_Ch05.pdf.

268 Boning, C. W., M. Scheinert, J. Dengg, A. Biastoch, and A. Funk, 2006: Decadal
269 variability of subpolar gyre transport and its reverberation in the North Atlantic
270 overturning. *Geophys. Res. Let.*, **Vol. 33**, L21S01.

271 Bryden, H. L., Longworth, H. L. & Cunningham, S. A., 2005. Slowing of the Atlantic
272 Meridional Overturning Circulation at 25°N. *Nature* **438**, 655-657..

273 Cubasch, U. *et al.* 2001. *Climate Change 2001: The Scientific Basis* (ed. Houghton, J.
274 T.) Ch 9, 525-585 (Cambridge Univ. Press, Cambridge, UK, 2001).

- 275 Cunninham S.A. and S. Alderson. 2007. Transatlantic temperature and salinity changes
276 at 24.5N from 1957 to 2004. *Geophys. Res. Lett.* 34, L14505.
- 277 Cunningham, S., Kanzow T., Rayner D., Baringer M.O., Johns W.E., Marotzke J.,
278 Longworth H.R., Grant E.M., Hirschi J.J-M., Beal L.M, Meinen C.S. and Bryden H.L.,
279 2007. Temporal Variability of the Atlantic Meridional Overturning Circulation at
280 26.5°N. *Science*, **317**,938-941.
- 281 Drijfhout, S. S. and W. Hazeleger, 2006: Changes in MOC and gyre-induced Atlantic
282 Ocean heat transport. *Geophys. Res. Let.*, **33**, L07707.
- 283 Eden C., and J. Willebrand, 2001: Mechanism of interannual to decadal variability of
284 the North Atlantic circulation. *J. Climate*, **14**, 2266-2280.
- 285 Ganachaud, A. & Wunsch, C.,2003. Large scale ocean heat and freshwater transports
286 during the World Ocean Circulation Experiment. *J. Clim.* **16**, 696-705.
- 287 Häkkinen, S. & Rhines, P. B., 2004. Decline of subpolar North Atlantic circulation
288 during the 1990s. *Science*, **304**, 555-559.
- 289 Ingleby, B. & Huddelston, M., 2006. Quality control of ocean temperature and salinity
290 profiles – historical and real-time data. *J. Mar. Sys.*,**65**,158-175.
- 291 Köhl A. and D. Stammer, 2007. Variability of the Meridional Overturning in the North
292 Atlantic from the 50 years GECCO State Estimation. The ECCO report series, 43.
293 Available at www.ecco-group.org.
- 294 Le Traon, P.-Y., F. Nadal, and N. Ducet.,1998. An improved mapping method of
295 multisatellite altimeter data. *J. Atmos. Oceanic Technol.*, **15**, 522-534.
- 296 Reynolds R., N Rayner, T Smith, D Stokes, W Wang., 2002. An improved in situ and
297 satellite SST analysis for climate. *J. Clim* , **15**, 1609-1625.

- 298 Vargas-Yáñez, M., Parilla, G., Lavin, A., Vélez-Belchi, P. & González-Pola, C., 2004.
299 Temperature and salinity increase in the eastern North Atlantic along the 24.5°N in the
300 last ten years. *Geophys. Res. Lett.*, **31**, L06210, doi:10.1029/2003GL019308.
- 301 Vellinga, M. & Wood, 2002. R. A. Global climatic impacts of a collapse of the Atlantic
302 thermohaline circulation. *Clim. Change* **54**, 251-267.
- 303 Wolff, J., E. Maier-Reimer and S. Legutke, 1997. The Hamburg Ocean Primitive
304 Equation Model. *Deutsches Klimarechenzentrum*, Hamburg, Technical Report No. 13.
- 305 Wunsch, C. & Heimbach, P., 2006. Estimated Decadal Changes in the North Atlantic
306 Meridional Overturning Circulation and Heat Flux 1993-2004. *J. Phys. Ocean.*, **36**,
307 2012-2024.

308

309

310 **Figures**

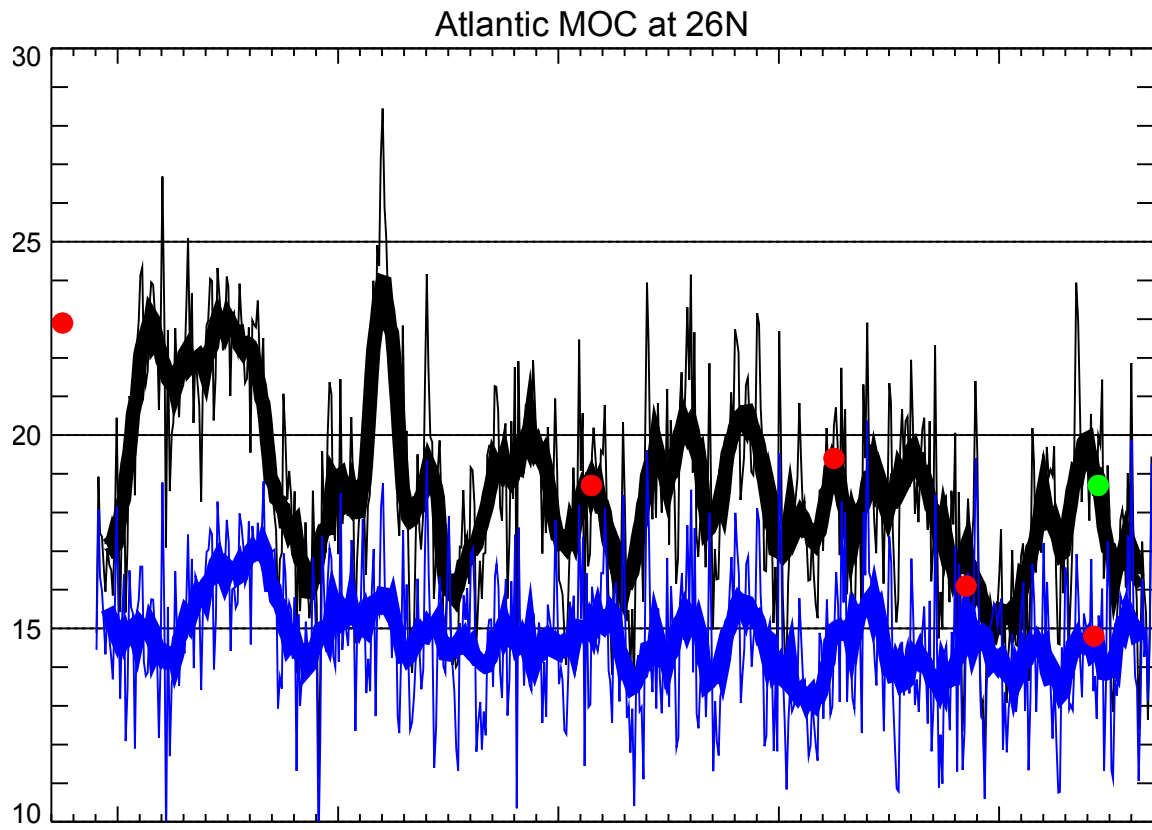


Figure 1 | Meridional overturning circulation (MOC) variability at 26°N. The time evolution of the MOC for both ORAS3 (black) and ORA-nobs (blue) is shown using monthly values (thin lines) and annual means (thick lines). Over-plotted are the annual-mean MOC values from BLC05 (red circles) and Cunningham et al 2007 (green circle).

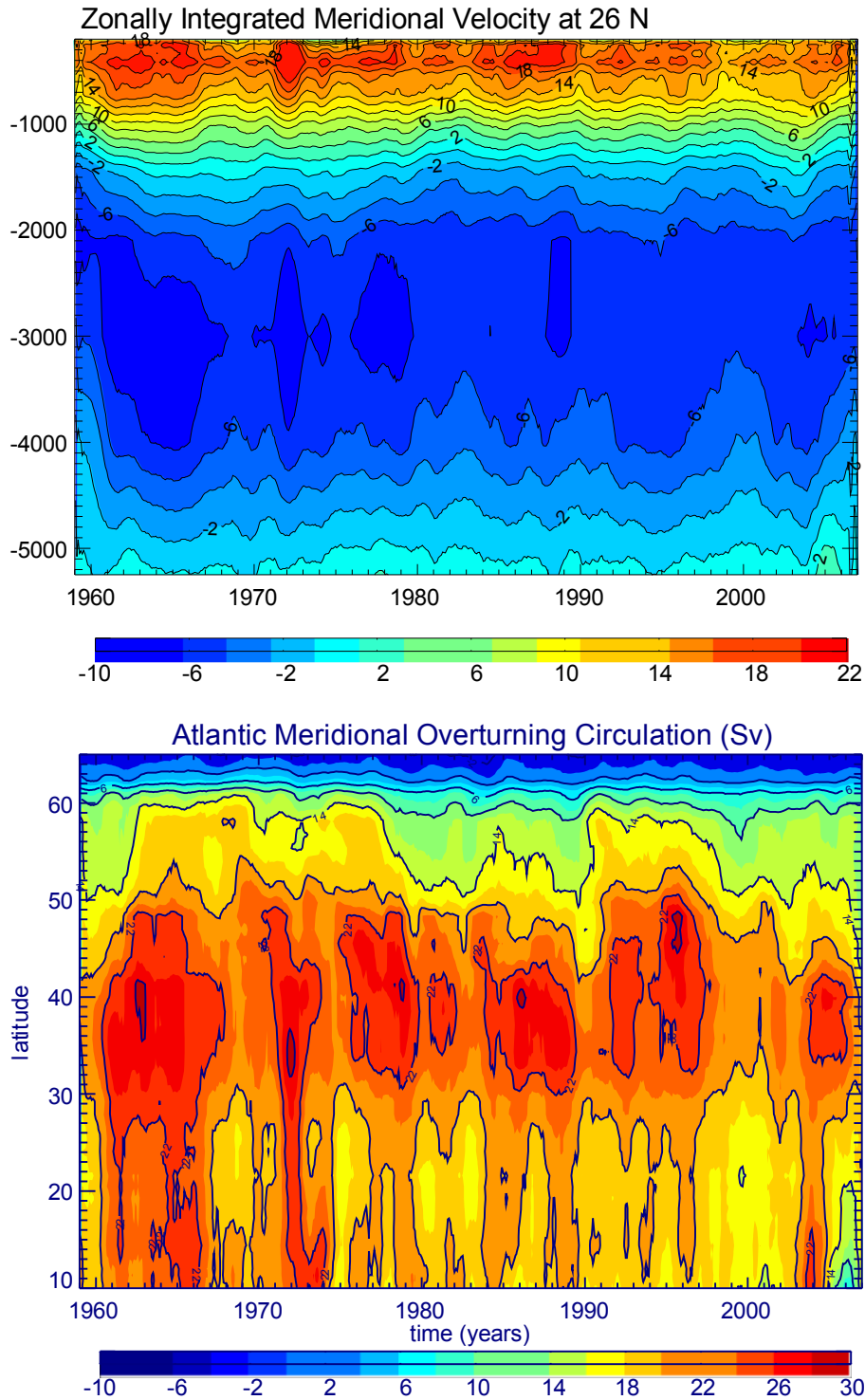
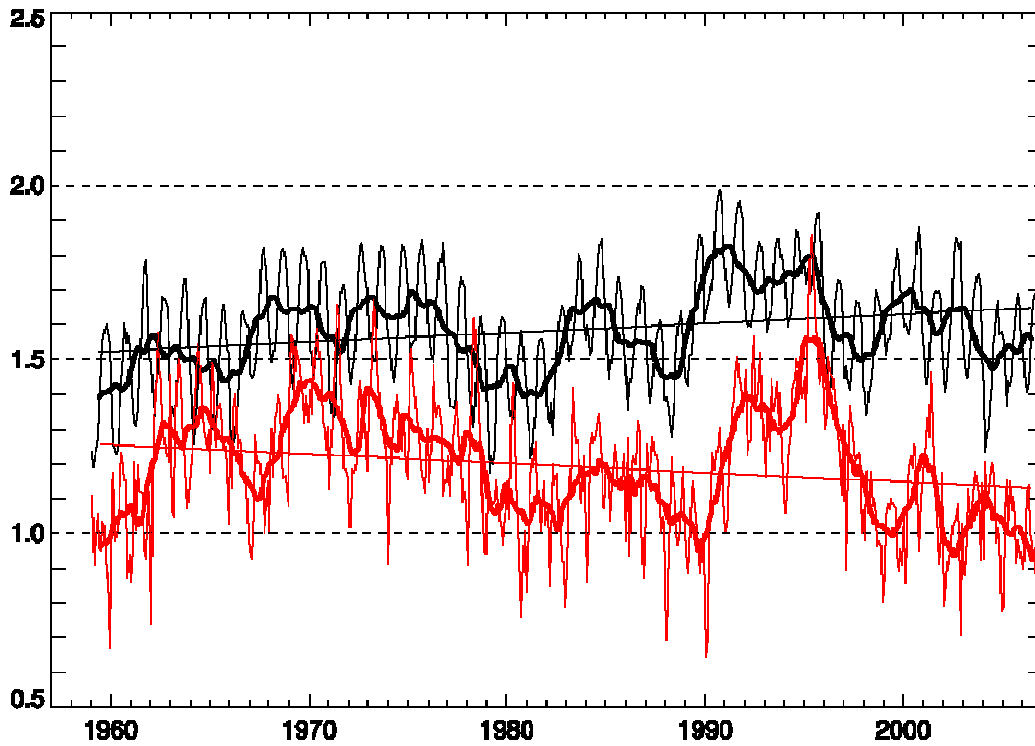


Figure2 | Vertical (a) and meridional (b) structure Atlantic MOC as a function of time. In (a) the vertical structure of the MOC is represented by the zonally integrated meridional velocity at 26°N, and units are $10^3 \text{m}^2/\text{s}$. Both the poleward transport within the upper 1000 m and the equatorward transports below 2000 m are decreasing with time. In (b), the MOC is calculated as the integrated meridional velocity above a reference depth of 1200m in units of Sv.



311

Figure 3 | Normalized timeseries of the subpolar gyre index (black) and MOC at 50N (red) from ORAS3. Overplotted are the linear trend estimates. The subpolar gyre index is computed as the sea level differences at 40N and 60N. The decrease in subpolar gyre intensity during the 90's is consistent with Hakkinen and Rhines 2004. The subpolar gyre variability leads the MOC variability at interannual time scales, but the trends are opposite.

312

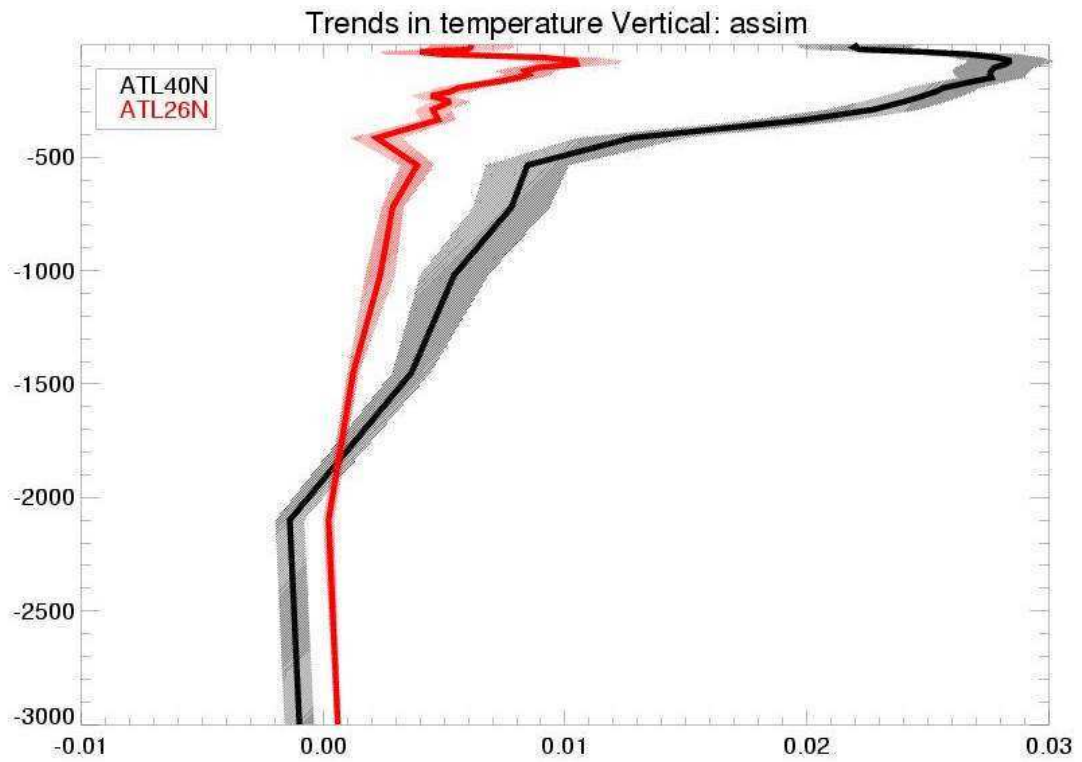


Figure 4 | Trends in the vertical temperature structure from the 48-year ORAS3 analysis, at 26°N (red) and 40°N (black). Units are K/yr. Shaded are the trend values within the 95% C.I.